Journal of the European Ceramic Society 20 (2000) 1345–1353

Relationship between flexural strength and surface roughness for hot-pressed Si_3N_4 self-reinforced ceramics

Yesha Zheng [a,*], Joaquim Manuel Vieira [a], Filipe José Oliveira [a], Joao Paulo Davim [b], Pedro Brogueira [c]

[a] *Departamento de Engenharia Cerâmica e do Vidro, Universidade de Aveiro, 3810 Aveiro, Portugal*
[b] *Departamento de Engenharia Mecânica, Universidade de Aveiro, 3810 Aveiro, Portugal*
[c] *Departamento de Física, Instituto Superior Técnico, Av. Rovisco Pais, 1096 Lisbon Codex, Portugal*

Received 28 June 1999; received in revised form 7 November 1999; accepted 12 November 1999

Abstract

The hot-pressed Si_3N_4 self-reinforced ceramics with Y_2O_3 and Al_2O_3 addition were first ground using the diamond wheel with the diamond grit of 64 μm size, and then polished using the diamond abrasives of 15, 6 and 1 μm size. The surface morphologies were examined by scanning electron microscopy (SEM) and atomic force microscope (AFM). The flexural strength at room temperature showed a net relationship with surface roughnesses (R_a, R_z, R_{3z}, R_t, R_q) the increase of which followed the surface finished and defect disappearance. The flexural strength and the negative square root of surface defect size, maximum peak-to-valley height of surface, fit the following equation: $\sigma_f = (A/R_t) - \left(B/\sqrt{R_t}\right) + C$, where surface compressive residual stress and defect size interact competitively on strength. Sharp peaks and deep grooves were undoubtedly the fracture origins after the first grinding by the diamond wheel. The obvious surface defects had been eliminated by the following polishing, where fracture may be initiated from subsurface defects; however, there was still some local damage observed by AFM due to diamond abrasion. The mirror finished surfaces should be stress free.

Keywords: Grinding; Roughness; Si_3N_4; Strength; Surfaces

1. Introduction

Due to their superior mechanical and thermal properties, structural ceramics such as Si_3N_4, SiC, Al_2O_3 and ZrO_2 have found increasing applications in high-temperature and high-stress situations, such as for turbine blades, automotive engine components, wear parts and cutting tools etc.[1–3] High dimensional accuracy and good surface integrity are usually required of these components. Although advances have been made in near net-shape technology, grinding with diamond wheels is still the machining method of choice.[4] The problems commonly found in ceramic grinding, however, are low grinding efficiency, surface–subsurface damage, strength degradation, low grinding ratio and high machining cost.[5] In the manufacture of high strength components, grinding alone may constitute a significant portion of the total cost.[6]

The most common method of machining these materials is grinding with a diamond tool. From the material's point of view this must be a very rough method, since diamond particles are forced into the surface. It is, therefore, not surprising that grinding causes decreased mechanical strength of the machined components, which has frequently been reported in the literature.[7–10] This reduction in strength is caused by cracks introduced into the surface layer during machining.[8–10] It has been shown that cracks perpendicular to the grinding direction are half-penny-shaped,[9,10] whilst those parallel to the grinding direction more or less continuously follow the grinding groove.[9,10]. The latter cracks seem to be deeper than the former[10] and they probably consist of halfpenny-shaped defects so close together that they in fact form an elongated crack.[9,10]

Ceramics are characteristically brittle and sensitive to the condition of the surface. The presence of cracks, pores, flaws and residual stresses at, or near, the surface, and the surface roughness determines the strength of the ceramic; for example, it may be reduced up to about 50%.[8]

* Corresponding author.
E-mail address: yesha@cv.ua.pt (Y. Zheng).

0955-2219/00/$ - see front matter
PII: S0955-2219(00)00018-2

In addition to mechanical grinding and lapping, methods such as ultrasonic, electro-discharge and laser machining are available.[11] The machining of ceramic components can be classified into two broad groups: (i) non-abrasive; and (ii) abrasive. Non-abrasive processes include ultrasonic machining and laser machining.[12] At present, the applications of non-abrasive machining methods are limited by one or more of the following features: (a) low material-removal rates; (b) poor surface finish; and (c) difficulty in controlling geometrical features such as straightness of cut.[2]

Abrasive machining processes generally involve superabrasive (most commonly, diamond) grinding wheels. Grinding with diamond wheels continues to be the predominant material-removal process for structural ceramics. Unfortunately, ground ceramics are known to have a strength-degradation problem caused by machining-induced damage.[8,13] The flexural strength of a ceramic part may often depend on the grinding parameters used to finish it.

Undoubtedly, past research results have contributed greatly to present knowledge of ceramic grinding processes. Conflicting observations also exist and there is need of more clarifying research work. Researchers are still striving to produce low-cost high-quality ceramic components. This implies that continuous effort is needed to better understand the physics and mechanical properties of ceramic grinding and finishing processes. As part of this continuous effort, particular emphasis was given in this study to the relationship of flexural strength and surface roughness for hot-pressed Si_3N_4 self-reinforced ceramics, which can lead to a clear quantitative understanding in this key effective factor.

2. Experiments

2.1. Material

The workpiece material used in this investigation was hot-pressed silicon nitride. Due to strong covalent bonds and low self-diffusivity of Si_3N_4, the classical solid-state sintering techniques are unable to densify the Si_3N_4. In order to densify the Si_3N_4, appropriate sintering aids must be used to promote liquid-phase sintering via solution–precipitation processes.[14] Y_2O_3 is a devitrification agent, stimulating the nucleation and growth of crystalline phases in the amorphous boundary. Al_2O_3 can reduce the softening temperatures of the residual amorphous phase.

The material composition is listed in Table 1. The material was uniaxially hot-pressed for 60 min at 1650°C under 25 MPa of offered pressure. The hot pressed pellets have the final density of 3.25 g/cm^3 after hot-pressing.

Table. 1
Hot-pressed Si_3N_4 composition

Composition	Si_3N_4	SiO_2	Y_2O_3	Al_2O_3
Mol%	85	8	4	3

The heating rate was controlled at 50°C/min from room–temperature to 1100°C, and 30°C/min to 1650°C, respectively.

Hot-pressed Si_3N_4 is representative of ceramics which are mechanically strengthened by the presence of elongated grains, so-called in-situ whiskers. Occasionally, exaggerated large grains are also observed. Fig. 1 shows this self-reinforced microstructure; the elongated grains impinged each other due to different growth rate in different growth direction, constituting a strong obstacle in front of the crack growth and resulting in self-reinforced microstructure, i.e. in-situ composite.

2.2. Grinding and polishing

All samples were pre-machined into flexural bars of 22~24 mm length and 3 × 4 mm mm^2 section. The grinding was done by a metal-bonded wheel of diamond sand of 64 μm with diameter (*d*) of 150 mm and width of 14.8 mm, wheel speed 44 m/s, and a depth of material removal of 10 μm. A copious supply of water-based coolant was consistently provided during the grinding operations. Grinding direction is parallel to the test bar major axis (longitudinal).

Polishing gives a reference state where material damage is minimized after previous lapping by reducing the diamond polish particle size stepwise from 15 to 6 μm, then to 1 μm, using diamond flat lapping/polishing machine, which can be automatically operated. Each step lasts until former defects and scratches are

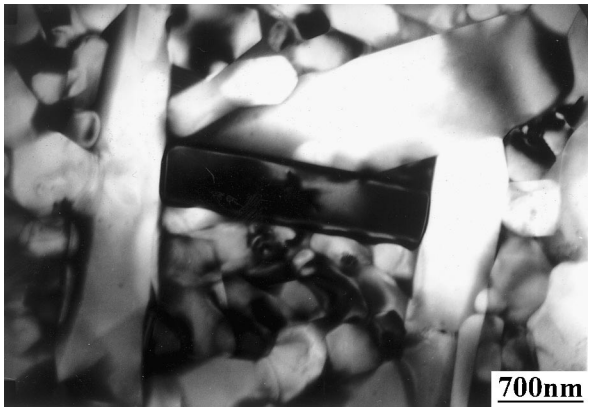

Fig. 1. The intercontact of elongated grains. This will become an enormous obstacle in the front of crack growth, so that the crack may suspend if the driving force of the crack tip is not enough to overcome this obstacle, resulting in the higher strength and toughness of the material. Therefore, this ceramic is called in situ composites or self-reinforced ceramics.

removed. All four faces of the test samples were finally polished to a mirror finish, where the majority of the roughness associated with the grinding had been removed by the polishing process. However, this procedure requires a vast amount of time. At least, 8∼20 samples of each type were tested in this key grinding and polishing programme.

To prevent failure caused by edge flaws, all the bars were chamfered prior to bending testing.

2.3. Three-point bend tests

The flexural strengths of the ground specimens were determined at room temperature using a three-point flexural testing facility. The span of the three-point bending fixture was 18 mm. The cross-head speed of the testing machine was 0.5 mm min^{-1}. At least 3∼8 specimens were tested for each condition.

2.4. Surface-roughness tests

Surface-roughness measurements were taken on the wide surface of the bend bars using a contact stylus-type probe made by Hommelwerke GMBH. Measurements were made along the length (L) of each test piece.

Roughness may be defined by many parameters: arithmetic mean roughness value (R_a); mean peak-to-valley height (R_z); averaged middle peak-to-valley height (R_{3z}); maximum peak-to-valley height (R_t); mean peak height value above the mean line (R_{pm}); single highest peak above mean line (R_p); root mean square roughness value (R_q); maximum profile depth (P_t).

The trace profiles of the grinding and the finishing surfaces recorded by roughness tester are shown in Fig. 2. The surface roughness of the ground specimens were measured in the range of 4.8 mm length so this, in fact, was the average data of macro-roughness (Table 2).

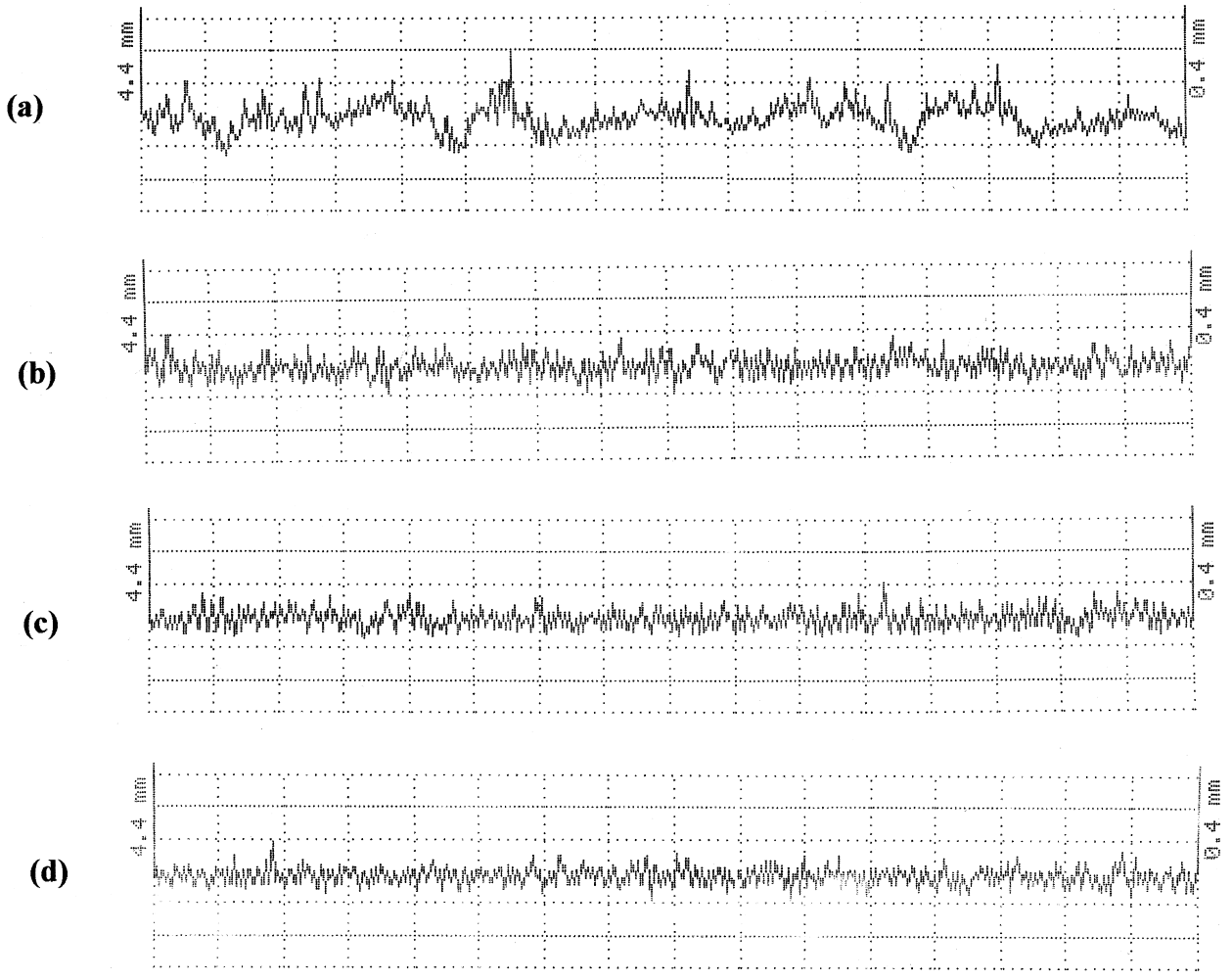

Fig. 2. Caption profiles of surface roughness by the roughness tester in 4.8 mm length; (a) after the first grinding using the diamond wheel of 64 μm size; (b) after the first polishing using the diamond abrasive of 15 μm size; (c) after the second polishing using the diamond abrasive of 6 μm size; (d) after the last polishing using the diamond abrasive of 1 μm size.

Table. 2
Relationship of surface roughness and bend strength for hot-pressed Si_3N_4 ceramics

Finish (μm)	Bend Strength (MPa)	R_a (μm)	R_z (μm)	R_t (μm)	R_{pm} (μm)	R_p (μm)	R_q (μm)	R_{3z} (μm)	P_t (μm)
64 (wheel)	869 ± 50	0.13	0.82	1.02	0.33	0.38	0.16	0.62	1.02
15	940 ± 35	0.06	0.45	0.52	0.22	0.24	0.08	0.37	0.52
6	1015 ± 25	0.04	0.24	0.35	0.15	0.18	0.05	0.25	0.35
1	116 ± 115	0.02	0.12	0.16	0.07	0.10	0.02	0.08	0.16

2.5. SEM observation

The ground surfaces were first examined by scanning electron microscopy. (SEM) inspection of the ground surface after the diamond wheel grinding suggested fragmented surfaces, indicating material removal predominantly by fracture mechanisms. Grinding tracks were evident and had very deep grooves. But SEM is only suitable to observe the surface of machined samples. It is not suitable for observation of the surface of polished samples. One must choose AFM to observe the surface morphology in range of the nanometer.

2.6. Atomic force microscope (AFM) observation

AFM (Nanoscope IIIa, Scanning Probe Microscope with Dimension 3100 Series digital instrument) was used to observed the surface morphology and roughness of ground and polished samples. Arithmetic mean roughness value (R_a) and root mean square roughness value (R_q) were obtained by AFM in the micro-range of 25 μm^2, which are listed in Table 3.

3. Results

3.1. Relationship between surface roughness and diamond abrasive size

Figs. 3 and 4 show the relationship of surface roughness and diamond grit size. Obviously, the surface roughnesses were largely improved by the grinding and polishing sequence, the surfaces of machined samples still have rough grinding grooves in Fig. 3(a). The top micrograph shows the rough groove after first grinding with a diamond wheel, but the surface finish has been largely improved by first grinding compared to the surface of the hot-pressed sample in the bottom of the graph [see Fig. 3(a)]. The grooves had been polished

Table. 3
Roughness R_a and R_q by AFM in the range of 25 μm^2 for ground and polished surface of Si_3N_4 ceramics

Diamond (μm)	As machined (64 μm)	15 (μm)	6 (μm)	1 (μm)
R_a	0.050	0.021	0.005	0.003
R_q	0.071	0.028	0.007	0.006

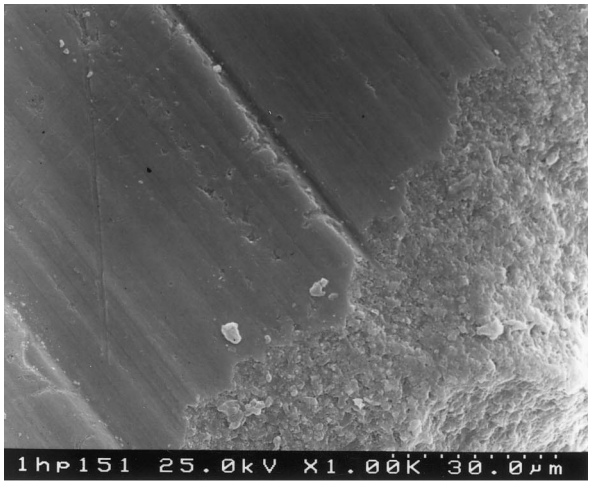

(a)

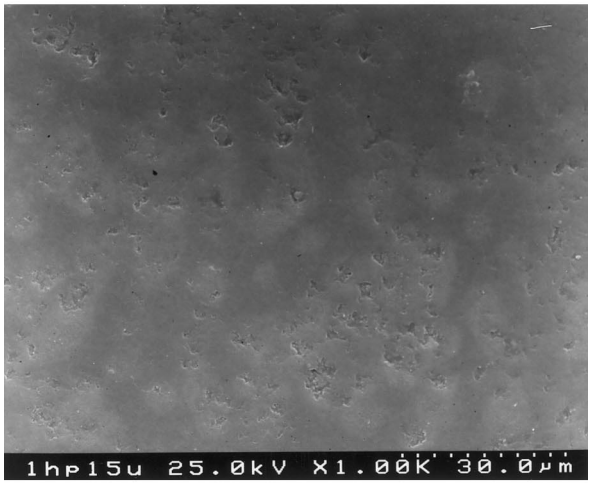

(b)

Fig. 3. SEM micrographs show surface morphologies of ground samples; (a) the rough and deep groove after first grinding using a diamond wheel (top of the photograph) and the initial rough surface in the as-sintered state (bottom of photograph); (b) surface flaws still survive the first polishing using 15 μm size diamond abrasive.

using the diamond grit of 15 μm size, but some flaws still remained on the surface [see Fig. 3(b)].

3.2. Relationship of surface roughness and flexural strength

Measurement shows a material-dependent effect of roughness on strength. Roughness measurements of ground samples parallel to the grinding direction show a clear correspondence between roughness and flexural strength. Fig. 5 shows the strong relationship between surface roughness (R_a) and flexural strength at room temperature, where the standard deviation of strength increases with the increase of surface roughness. Because strength is closely related to the surface flaw sizes, the standard deviation of strength values decreases with the improvement of surface quality (Fig. 5). Fig. 5 shows that the positive deviations of flexural strength in the high roughness samples are often inside the range of strengths of the lower roughness ones except for the last polishing.

As a result of minimized machining defects, Si_3N_4 samples reach the same level of their highest strength values of 1161.1 MPa reported to date (see Fig. 5 and Table 3).

3.3. Relationship of flexural strength and diamond abrasive size

Sections 3.1 and 3.2 have proved the relationship between surface roughness and diamond abrasive size, and between flexural strength and diamond abrasive size, respectively. In fact, from the above results there has been an equally good trend between flexural strength and diamond abrasive size (see Fig. 6). The flexural strengths were largely improved as abrasion diamond sizes were decreased from 15 to 1 μm. It is illustrated that surface defects often are fatal origin of fracture in ceramics and the strength of ceramics can be largely improved by grinding and finishing the surface, removing hidden danger from the surface. But noticeably, we would rather use the relationship of strength and roughness than that of strength and diamond abrasive size here. Why? There is a very direct correlation between strength of ceramics and surface damage than that between strength and diamond abrasive size. It is necessary to finish off traces remaining from the last grinding. This is not only a very cautious work but also consumes process time, or else it cannot be expected to obtain an equally good trend between the strength and diamond abrasive size.

3.4. Surface morphology by SEM and AFM

Fig. 7(a) clearly shows the surface morphology of samples after first grinding by diamond wheel. There still are sharp peaks and valleys in the surface of first grinding by diamond wheel. SEM observation also

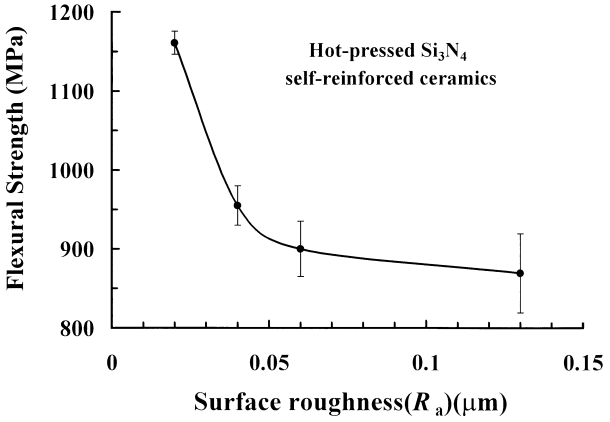

Fig. 5. The effect of surface roughness, R_a and R_q in the longitudinal directions, on the flexural strength of the hot-pressed Si_3N_4 self-reinforced ceramics.

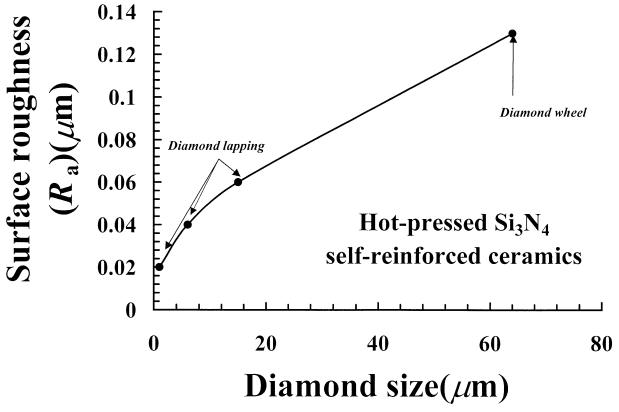

Fig. 4. Relationship of surface roughness and diamond abrasive size for the grinding and polishing of hot-pressed silicon nitride.

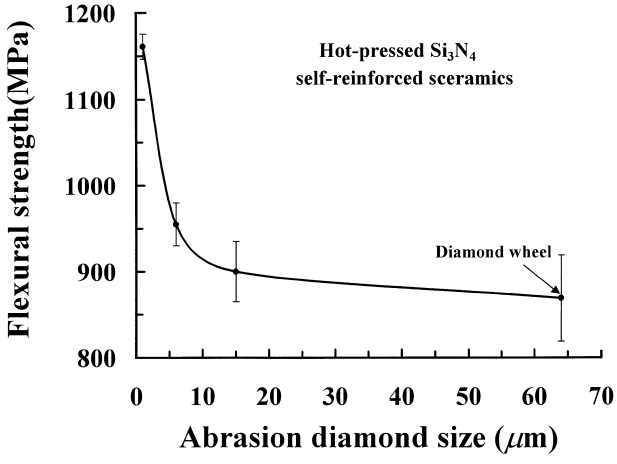

Fig. 6. The effect of diamond abrasive size on the flexural strength in the hot-pressed Si_3N_4 self-reinforced ceramics.

shows the deep grooves (Fig. 8), which will undoubtedly become the origin of fracture. By diamond grit of 15 μm size the sharp peaks of sample surface become polished, but some valley still remain [Fig. 7(b)]. Some grinding marks and small grit particles on the surface survived the 6 μm polishing [see Fig. 7(c)]. The 1 μm polishing had completely polished all features on the surface, but left some marks of grinding grit surface damage [Fig. 7(d)]. The cracks parallel to the grinding direction are more elongated and deeper than those perpendicular to the grinding direction (see Figs. 7 and 8).

3.5. Flaw size and strength

The surface roughness parameter R_t is a direct measure of the maximum crack or pit depth in the surface, and hence the flaw size c is equated to R_t here.

The plot of fracture stress σ_f against the roughness (R_t), expressed as $(R_t)^{-1/2}$, is a useful representation which highlights a surface geometry-controlled limit (see Fig. 9). The curve of the strength of ceramics fits the following equation:

$$\sigma_F \frac{A}{R_t} - \frac{B}{\sqrt{R_t}} + C \tag{1}$$

where A, B, and C are constant, which is only related with material properties and test condition. The surface energy per unit area (γ) and the elastic modulus (E) should have been included in A, B and C coefficients. $A=92.3$, $B=127.6$ and $C=903.4$ for the hot-pressed Si_3N_4 self-reinforced ceramics of this study.

According to Eq. (1), the curve has a minimum limited value, where the interaction of compressive residual stress and the defect size in surface layer reach balance. This is rational, because compressive residual stress usually make a positive contribution and defect size conversely. Diamond particles are forced into sample surface, resulting into both surface compressive residual stress and defect size, both of which increase with increase of wheel power. Compressive residual stress depresses and delays propagation of flaw crack in left of curve and the finer surface improve material strength although surface has only weak or free stress layer in the

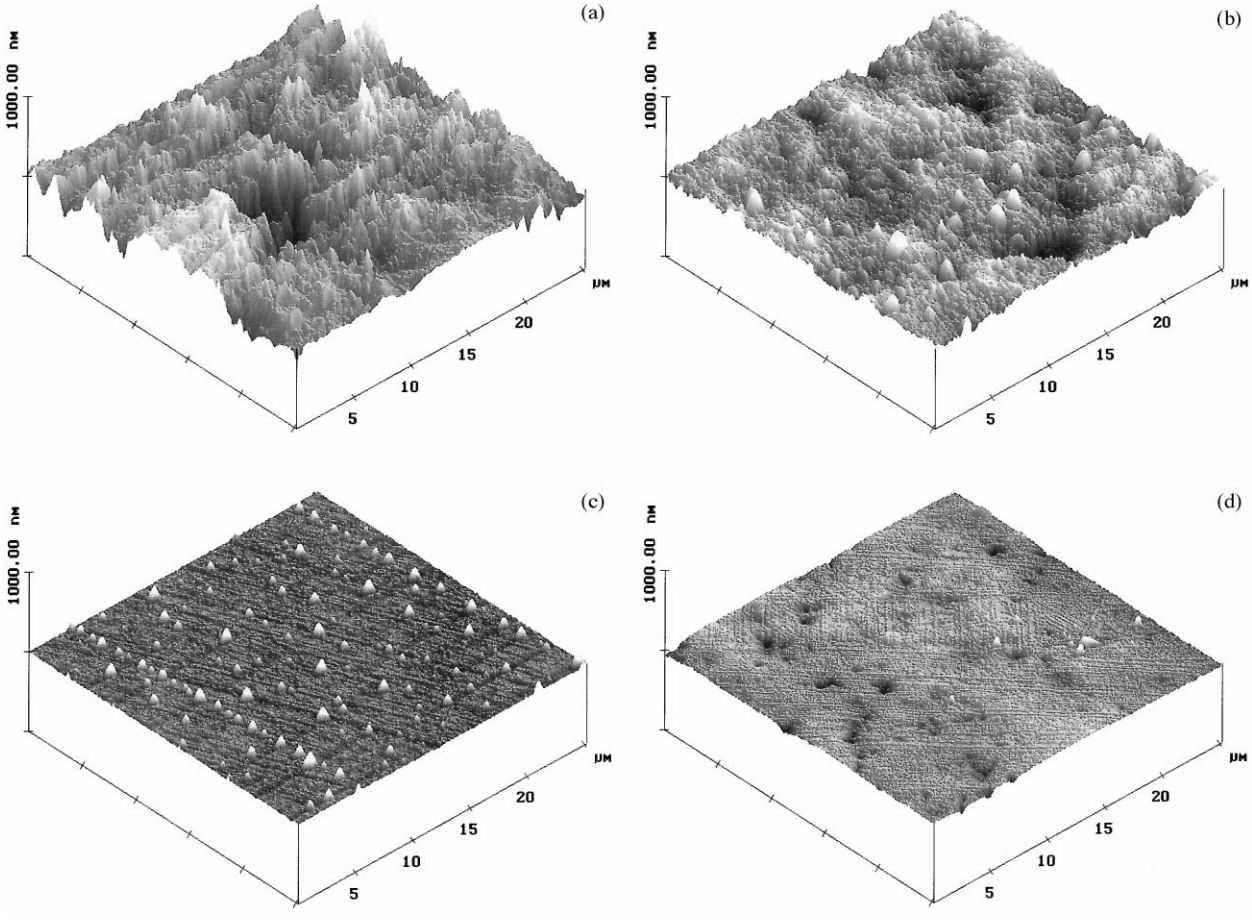

Fig. 7. AFM micrographs of surface morphologies in 25 μm^2 area; (a) after the first grinding using the diamond wheel of 64 μm size; (b) after the first polishing using the diamond abrasive of 15 μm size; (c) after the second polishing using the diamond abrasive of 6 μm size; (d) after the last polishing using the diamond abrasive of 1 μm size.

right of curve, here two mechanisms together restrict material quality (Fig. 9). The range of R_t size is also limited, and it is impossible for R_t to be decreased unlimited, because fracture strength will be controlled by the pores and subsurface flaws in the bulk, if the surface flaws have been completely eliminated.

4. Discussion

4.1. Difference of surface roughness by two methods

Tables 2 and 3 show the roughness values measured by machine contact pin and AFM, respectively. The former values were higher than that of the latter. The former has an advantage: its values were in fact the average ones in the range of 4.8 mm length; the disadvantage is: it cannot detect some micro-valleies, as only some macro-valleies can be contacted. The latter advantage: its values were obtained by non-contact AFM detection, which was in fact more accurate measurement from all micro-details; the disadvantage: the detection resulted only from very local area, such as the range of 25 μm^2.

The present authors consider it practical to use machine-contact pin in long range for engineering components if the surface roughness is required to be measured. But it should be recommended to take as much areas as possible as AFM is used in scientific research. AFM was adopted in this article only in order to observe surface morphologies, i.e. for a non-quantum aim.

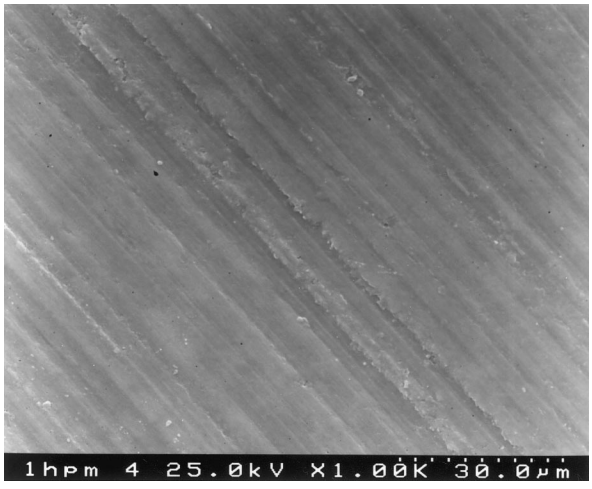

Fig. 8. SEM micrograph of the deep groove of the ground surface after the first grinding using the diamond wheel of 64 μm size; the large groove is parallel to the grinding direction.

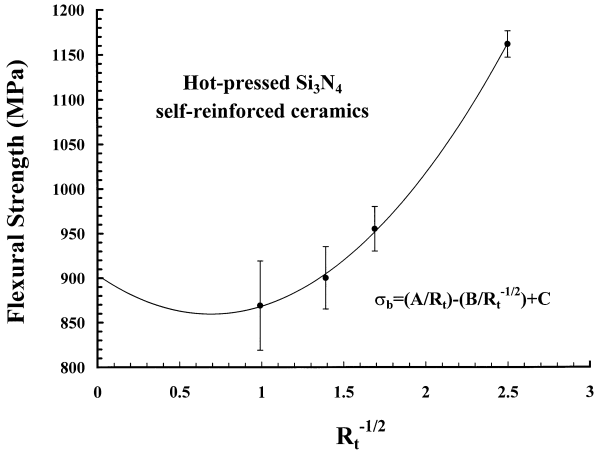

Fig. 9. Flexural strength as a function of surface roughness parameter, $R_t^{-1/2}$, which is a direct measure of the maximum peal-to-valley height, in fact, the maximum crack or pit depth in the surface.

4.2. Residual compressive stresses

Murata et al. (1992).[15] had proposed that the depth of the compressive residual stress can be estimated from the plastic deformation zone obtained by sphere indentation, which gives an analogous effect to the burnishing action of the abrasive grains. The depth of the compressive residual stress, d, is given as:

$$d = (0.6 \sim 0.8) r^{1/3} Rz_y^{2/3} (E/H)^{2/5} \quad (2)$$

where r is the average radius of the abrasive grains, Rz_y is the five-point average peak-to-valley height of the ground surface in the direction perpendicular to the grinding direction, E is the young modulus and H the hardness. According to Eq. (2), the calculated values of d, the depth of residual compressive stress, as a function of Rz_y, according to Eq. (2) are shown in Fig. 10. The depth of the effective layer of residual stress is below 2 μm for the diamond abrasive grains finer than that of 6 μm size. In fact, the deep stress layer produced by using the diamond wheel had first been ground by the following polishing steps. The polished surface, however, should be stress free only under the mirror polish conditions.

Several similar calculations were made and they all show that grinding had resulted in a compressive surface layer.[16,17] This is a positive effect that would increase the material strength. It may help to close cracks and delay the onset of crack propagation, particularly in restraining the subsurface crack growth.

The polished surface is almost free of residual stresses. Since the rough surface layer has been ground, the residual stresses are kept inside a very thin hardened layer. A large part of finely polished samples should be free of residual stresses in the present study.

4.3. Fracture stresses associated with flaw size

Pre-existing cracks have long been recognized as precursors to failure.[18–22] The strength of materials is

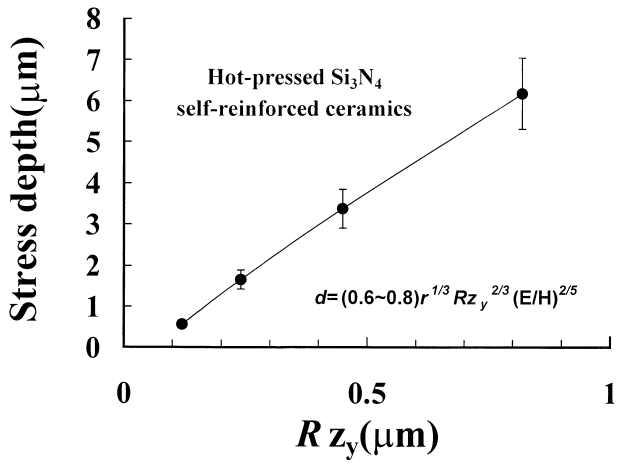

Fig. 10. Depth of residual compressive stress layer versus R_{zy}, the five-point average peak-to-valley height of the ground surface.

obviously related to flaw size. Flaws are divided into surface, corner, subsurface and internal defects, such as surface scratch, groove and internal pore, inclusion, microcrack, etc. Fatal cracks often originate from surface microdefects in the centre sites beneath surface of bending samples, where the bending sample bears the maximum tensile stress. So the flexural strengths can largely be improved by finely finishing the surface. Secondly, it was observed that the specimens often failed from corner cracks, if the surface beneath has been perfectly finished, where stresses often concentrate more, and corners are chamfered round rather at 45°. Thirdly, the fracture origins also often initiate from subsurface flaws of the well polished samples, resulting from bulk defects that are produced during the sintering process, such as pore, inclusion and microcrack, etc. The above results were deduced from a large number of SEM micrographs in fracture origins (SEM photographs are omitted here due to space).

Eq. (1) only describes the relationship of flexural strength and surface maximum flaw size [maximum peak-to-valley height (R_t)], since flaw and flaw size beneath the surface of bending samples are the key factors of strength dependence in ceramics, which is also the focal point discussed in this paper. The classic fracture mechanics were based on an internal, penny-shaped crack of radius c being first introduced prior to loading, which is completely unsuitable for discussion in this paper. Fracture stresses are usually related with negative square root of internal flaw size in the original Griffith and its modification equations,[18–22] which just discussed the effect of internal flaws. Firstly, the effect of beneath the surface flaws is even more prominent in the bending test of brittle solid in this paper. Secondly, self-reinforced Si_3N_4 ceramics have an elongated grain morphology, and its critical strain energy release rate is four times larger than for the same material with an equiaxed grain morphology.[19] So, it is not realistic to explain this especial engineering application only using classic fracture mechanical formulas. Eq. (1) accords well with the test results in this paper when compared with the numerous equations of fracture mechanics existing to date. It should be of great importance in the ceramic community, especially regarding design and reliability analysis of ceramic components.

4.4. Fracture toughness associated with crack growth

Strength and fracture toughness cannot only be integrated but are also contradictory in some conditions. For example, the flexural strength could be obviously improved by surface fine finishing, but fracture roughness did not show obvious improvement in this test (the data of fracture toughness were omitted here), because the former depends on crack initiation and the latter depends on crack growth. Surface finishing eliminated the hidden danger of surface crack initiation although, of course, strength was improved. But it did not have direct connection with crack growth, so fracture toughness virtually almost did not change.

4.5. Microplasticity produced by local stress concentration

The observed effect of microplasticity is a common feature in macroscopically brittle materials. Unequivocal evidence of plastic flow for grinding of single crystals and polycrystalline alumina was obtained by transmission electron microscopy (TEM) which showed the finished surface after grinding to contain dense dislocation arrays.[23] Similar findings were reported for grinding of MgO single crystals.[24]

High stresses applied in small-scale microstructural volumes by processes such as machining, abrasion, friction and wear give rise to microplastic deformation processes taking place in these ceramics, which are known as brittle materials. The elastic/plastic interaction of abrasive grains with the ceramic surface is considered to be analogous to a series of closely-spaced, high-speed, sliding single-point indenters. The trace of plastic deformation due to local high stresses of a diamond wheel can be observed from the side of a deep groove (Fig. 8).

In summary, the material removal process associated with grinding is probably primarily a series of localised surface fractures, whereas with lapping and polishing tend to be predominantly a ductile or plastic processes: those latter processes are capable of producing a smooth surface finish and are beneficial as post-grinding processes.

5. Conclusions

1. The flexural strengths at room temperature of Si_3N_4 self-reinforced ceramics correlates to the

surface roughness (R_a,R_z,R_{3z},R_t,R_q) of samples ground and polished by using diamond abrasive. The flexural strengths are obviously improved with decrease of flaw sizes. The dependence of flexural strength at room temperature on flaw size, R_t, as given by the maximum peak-to-valley height R_t, is given by the following relationship:

$$\sigma_f = \frac{A}{R_t} - \frac{B}{\sqrt{R_t}} + C$$

Flexural strength is actually interacted by both compressive residual stress and defect size in the surface layer.

2. SEM and AFM obversations show that the sharp peak and valley, groove all are fatal fracture origin after the first grinding using diamond wheel; the fracture origin may initiate from the subsurface after the following fine polishing using diamond abrasive of 6 and 1 μm, where the sharp peak, valley and groove had been grinded, but the surfaces had the mark of micro-damage by diamond grit.
3. Flexural strength can be achieved 1161 MPa after fine grinding using the diamond abrative of 1 μm size for this hot-pressed self-reinforced Si_3N_4 ceramics.

Acknowledgements

This work was supported by UIMC-Research Unit of Ceramic Materials, Praxis Contract No.53, and by Foundation for Science and Technology, Lisbon, Portugal under Praxis XXI/BPD/18876/98 contract, to which the authors would like to express sincere acknowledgement.

References

1. Schwartz, M. M., *Handbook of Structural Ceramics*. McGraw-Hill, New York, 1992.
2. Bandyopadhyay, B. P., The effects of grinding parameters on the strength and surface finish of two silicon nitride ceramics. *J. Mater. Proc. Tech*., 1995, **53**, 533–543.
3. Maksoud, T. M. A., Morgan, J. E., Fox, T. G. and Scott, J. A., Grinding of ceramics: the effect on their strength properties. *J. Mater. Proc. Tech*., 1994, **43**, 65–75.
4. Jahanmir, S., Ives, L. K., Ruff, A. W. and Peterson, M. B., *Ceramic Machining: Assessment of Current Practice and Research Needs in the United States*. NIST Special Publication, June 1992, p. 834.
5. Li, K. and Liao, T. W., Modelling of ceramic grinding processes Part I. Number of cutting points and grinding forces per grit. *J. Mater. Proc. Tech*., 1997, **65**, 1–10.
6. Malkin, S. and Ritter, J. E., Grinding mechanisms and strength degradation for ceramics. *J. Eng. Ind*., 1989, **111**, 167.
7. Rice, R. W., The science of ceramic machining and surface finishing I. In *National Bureau of Standards Special Publication 348*, ed. S. J. Schneider and R. W. Rice. US Government Printing Office, Washington DC, 1972, pp. 365–481.
8. Wu, C.Cm. and Mckinney, K. R., The effect of surface finishing on the strength of commercial hot pressed Si_3N_4. In *Symposium on the Science of Ceramic Machining and Surface Finishing II*, ed. B. J. Hockey and R. W. Rice. National Bureau of Standards SP562, Washington, DC, 1979, pp. 477–481.
9. Marshall, D. B., Progress in nitrogen ceramics. In *NATO ASI series E*, ed. F.L. Riley. Martinus Nijhoff Publishers, Haag, 1983. p. 635
10. Hakulinen, M., Residual strength of ground hot isostatically pressed silicon nitride. *J. Mater. Sci*., 1985, **20**, 1049–1060.
11. Konig, W. and Wemhoner, J. Adapted machining routes for ceramic components. *Proc. German Ceram. Soc*., 1986–87, **1**, 21–49 (in German).
12. Firestone, R. F., Abrasionless machining methods for ceramics. In *Symposium on the Science of Ceramic Machining and Surface Finishing II*, NBS Publication **562**,1979, pp. 261–281.
13. Anon. *Surface Texture (Roughness, Waviness and Lay),* ANSI Standard B46 1. ASME, New York, 1985.
14. Ota, M. and Miyahara, K., The influence of grinding on the flexural strength of ceramics. *SEM Tech. Paper*, 1990, **MR90**, 538.
15. Murata, K., Mizutani, K. and Tanaka, Y., An approach to residual stress in the ground layer of ceramics from material removal by grinding. *J. Soc. Mater. Sci., Jpn*, 1992, **41**(464), 624–630.
16. Lange, F. F., James, M. R. and Green, D. J., *J. Am. Ceram. Soc*., 1983, **66**, C–16.
17. Li, K. and Liao, T. W., Review: surface/subsurface damage and the fracture strength of ground ceramics. *J. Mater. Proc. Tech*., 1996, **57**, 207–220.
18. Griffith, A. A., *Phil Trans. Roy. Soc., (Lon.)*, 1920, **221A**, 219.
19. Lange F. F., Origin and use of fracture mechanics. In: *Fracture Mechanics of Ceramics*, ed. R. C. Bradt, D. P. H. Hasselman and F. F. Lange. ISBN 0-306-37591-5, 1993, pp. 3–16.
20. Wolf, K., *Z. Angew Math. Mech*, 1923, **3**, 107.
21. Sack, R. A., *Proc. Phys. Soc., (Lon.)*, 1946, **58**, 729.
22. Sneddon, I. N., *Proc. Phys. Soc., (Lon.)*, 1966, **187A**, 229.
23. Hockey, B. J., Observations on mechanical abraded aluminium oxide crystals by transmission electron microscopy. *The Science of Ceramic Machining and Surface Finishing*. NBS Special Pub. 348, 1972, p. 333.
24. Koepke, B. G. and Stokes, R. J., A study of grinding damage in magnesium oxide single crystals. *J. Mat. Sci*., 1970, **5**, 240.